Available online at www.sciencedirect.com
SCIENCE DIRECT®
Journal of Catalysis 236 (2005) 80–90
JOURNAL OF CATALYSIS
www.elsevier.com/locate/jcat

Selective hydrogenation of α,β-unsaturated ketone to α,β-unsaturated alcohol on gold-supported iron oxide catalysts: Role of the support

C. Milone [a,*], R. Ingoglia [a], L. Schipilliti [a], C. Crisafulli [b], G. Neri [a], S. Galvagno [a]

[a] *Department of Industrial Chemistry and Materials Engineering, Faculty of Engineering, University of Messina, Contrada di Dio, I-98166 Messina, Italy*
[b] *Department of Chemistry, University of Catania, Viale A. Doria 5, I-95100 Catania, Italy*

Received 28 June 2005; revised 14 September 2005; accepted 14 September 2005

Available online 18 October 2005

Abstract

The influence of the structural characteristics of the support in the liquid-phase reduction of *trans*-4-phenyl-3-buten-2-one or benzalacetone (C_6H_5–CH=CH–CO–CH_3) to the corresponding α,β-unsaturated alcohol (UA) on gold-supported iron oxide catalysts was investigated. Commercial goethite [FeO(OH)], maghemite (γFe_2O_3), and hematite (αFe_2O_3), along with an iron oxy-hydroxide prepared by precipitation, were used as supports. The catalytic behavior of Au/Fe_2O_3 reference catalyst (supplied by the World Gold Council) was also investigated. Gold-supported catalysts and the parent supports were extensively characterized by BET, X-ray diffraction, temperature-programmed reduction, and transmission electron microscopy. On all gold catalysts except the Au/Fe_2O_3 reference, the catalytic activity increased with increasing gold content. The lowest activity of reference with respect to the catalyst with a similar gold loading has been ascribed to the different sample pretreatments. Samples prepared by us were reduced under very mild conditions (in H_2 at 343 K for 1 h), whereas the Au/Fe_2O_3 reference was calcined at 773 K. From our data, no correlations can be drawn between activity and selectivity and mean gold particle size. Selectivity toward the hydrogenation of the conjugated C=O bond varied with the structural characteristics of the support, ranking in the order FeO(OH) > iron oxy-hydroxide > γFe_2O_3 > αFe_2O_3. On the most selective catalyst—gold supported on goethite—the selectivity toward the formation of UAs was 64%. A correlation between the reducibility of catalysts and selectivity was found. Selectivity toward the formation of UA increased with the reducibility of the support. In accordance with data in the literature, we propose that an electron transfer from the reduced support to the metal creates more electron-enriched gold particles on which the back-bonding with the π^* C=O orbital is favored, so that the hydrogenation of the C=O group increases over that of the C=C group. However, it cannot be ruled out that the enhancement of the selectivity is favored through a cooperative effect of special Fe(III) or Fe(II) sites, and that more negatively charged gold nanoparticles nearby present the reduced support.

Keywords: Gold catalysts; Selective hydrogenation; α,β-Unsaturated ketones; α,β-Unsaturated alcohols; Iron oxide

1. Introduction

Recent studies have widely reported that gold-supported catalysts show a remarkable selectivity toward the hydrogenation of the conjugated C=O bond in the hydrogenation of α,β-unsaturated aldehydes [1–5] and ketones [6,7]. The catalytic behavior of gold in the hydrogenation of the α,β-unsaturated ketones is of a particular relevance from both a scientific and a synthetic standpoint, due to the fact that the selective hydrogenation of these substrates by gaseous H_2 in the presence of heterogeneous catalysts is very difficult [8], although it can be easily achieved under hydrogen transfer conditions [9,10]. The reduction of lactonic enone, an intermediate in the prostaglandin synthesis, to secondary allylic alcohol occurs with high yields on Pt–Sn supported on SiO_2 catalysts, using isopropyl alcohol as a hydrogen donor [10]. Catalysts contain alloyed Pt–Sn particles covered by oxidized forms of tin at the surface, together with ionic tin on the support. It has been suggested that the high selectivity in the hydrogenation of lactonic enone is the result of decreased adsorption of C=C bond on Pt–Sn alloyed particles, activation of carbonyl on the oxidized Sn ions, and the use of hydrogen transfer agent, which favors a lower hydrogen coverage with respect to gaseous hy-

* Corresponding author.
E-mail address: cmilone@ingegneria.unime.it (C. Milone).

0021-9517/$ – see front matter
doi:10.1016/j.jcat.2005.09.023

drogen [10]. Another factor contributing to the enhanced hydrogenation rate of the conjugated C=O bond is steric hindrance at the C=C bond of the prostaglandin-type unsaturated ketone. The importance of steric hindrance at the C=C bond has been confirmed by experiments carried out with methylvinylketone, which, under similar reaction conditions, was reduced mainly to saturated ketone [10].

Recently, De Bruyn et al. [11] reported on the chemoselective reduction of complex α,β-unsaturated ketones to unsaturated alcohol (UA) over Ir-supported catalysts. A number of substrates, (steroid enones, prostaglandin intermediates, α-ionone, and β-ionone) with varying degrees of substitution on the conjugated C=C bond have been investigated. The reductions were carried out in the liquid phase at 298 K in the presence of gaseous H_2. On all of the substrates but the prostaglandin intermediates, the chemoselective reduction of enones to allylic alcohol occurs when isopropyl alcohol (secondary alcohol) or isoamyl alcohol (tertiary alcohol) are used as solvents. The use of methanol (primary alcohol) leads to the preferential hydrogenation of the C=C bond with formation of saturated ketone. Among the catalysts investigated, Ir supported on β-zeolite are more selective toward hydrogenation of the conjugated C=O bond. Ir supported on C and TiO_2 also show higher selectivity (>45%) in the hydrogenation of α-ionone using isopropyl alcohol as a solvent [11]. In contrast, in earlier work, Kaspar et al. [8] found that Ir/TiO_2 catalyst showed no selectivity in the gas-phase hydrogenation of mesityl oxide (4-methyl-3-penten-2-one).

A peculiarity of gold is its intrinsic selectivity toward hydrogenation of the conjugated C=O bond using gaseous H_2 as a reductant. We have previously verified that during the liquid-phase hydrogenation of several substrates, including *trans*-4-phenyl-3-buten-2-one (benzalacetone), 4-methyl-3-penten-2-one, and 3-penten-2-one, the reduction occurs by means of molecular H_2, and the mechanism of hydrogen transfer from the alcohol to the substrate does not occur [7].

In the liquid-phase hydrogenation of benzalacetone on gold supported on Al_2O_3, the selectivity toward the formation of UA approaches 10%; a strongly enhanced selectivity (>60%) has been obtained on gold supported on iron oxide catalysts [7]. Moreover, it has been pointed out that iron oxide by itself is not sufficient to enhance the hydrogenation rate of C=O with respect to the C=C bond in hydrogenation of the α,β-unsaturated ketones—both gold and iron oxides are necessary. Indeed, when the hydrogenation of benzalacetone was carried out on catalysts prepared by dispersing colloids of metallic ruthenium on the same iron oxide support used to disperse gold, the selectivity of UA was <2% [7]. This indicates that the catalytic behavior arises from a synergetic effect between the two constituents.

It has been argued that the intrinsic selectivity of gold can be due to the adsorption mode of the conjugated systems on this metal. Some have proposed that among the different adsorption modes of the conjugated systems [12,13], gold is likely a metal on which the 1,2-C=O adsorption mode is preferred over the 1,4-C=C–C=O mode. The scarcity of the 1,4-C=C–C=O species on gold catalysts, which are responsible for the formation of saturated aldehydes or ketones [12,13], is in accordance with the higher intrinsic selectivity of gold catalysts toward the formation of UA.

In the hydrogenation of benzalacetone, selectivity to UA is strongly influenced by the microstructural characteristics of the iron oxide support. Gold supported on amorphous oxyhydroxides or on a partially crystallized mixture of goethite [FeO(OH)], ferrihydrite, and hematite (αFe_2O_3) is more selective than gold supported on well-crystallized hematite [7].

The aim of the present work is to gain a deeper insight into the role of the support in the catalytic behavior of gold catalysts in the hydrogenation of benzalacetone. Consequently, we investigated the catalytic activity of gold catalysts supported on single-phase iron oxides, including goethite, maghemite (γFe_2O_3), and hematite, and also of gold supported on a mixture of goethite, ferrihydrite, and hematite. We performed a detailed characterization of the catalysts to clarify the nature of the active sites.

2. Experimental

2.1. Sample preparation

Au-supported catalysts were prepared by deposition-precipitation in accordance with Haruta's procedure [14]. The deposition-precipitation of gold onto the supports was done by adding the support to an aqueous solution of $HAuCl_4$ previously adjusted at pH 7–8 with NaOH. The slurry was maintained at 343 K, under vigorous stirring, for 2 h. Then the samples were filtered, washed with deionized water until chloride was eliminated, and dried under vacuum at 353 K for 1 day.

Goethite, maghemite, and hematite used as supports were commercial products purchased from Aldrich. An iron oxyhydroxide support was prepared by precipitation of iron hydroxide from a solution of $Fe(NO_3)_3{\cdot}9H_2O$ (Fluka) as starting materials. The precursor was poured into an aqueous solution of Na_2CO_3, 1 M (pH = 11.9) and maintained at 353 K under vigorous stirring. The solid was digested overnight at room temperature, washed with water until free of chloride ions ($AgNO_3$ test), then dried under vacuum at 353 K for 1 day.

The gold content was determined by measuring the absorbance of gold solutions at $\lambda = 400$ nm [15]. The solutions were prepared by dissolving the catalysts in HCl–HNO_3 (3:1 by volume), then adding a solution of tin(II) chloride in hydrochloric acid.

2.2. Sample characterization

Surface area measurements were made using the BET nitrogen adsorption method in a conventional volumetric apparatus, after outgassing (10^{-4} mbar) the sample at 353 K for 2 h. X-ray diffraction (XRD) studies were carried out with an Ital-Structures diffractometer using nickel-filtered Cu-K_α radiation by mounting the powder samples on Plexiglas holders. Diffraction peaks were compared with those reported in the JCPDS Data File.

Temperature-programmed reduction (TPR) experiments were carried out in a conventional apparatus, heating the sample (weight = 0.05 g) from room temperature to 800 K (at a rate of 10 K/min) under 5% H_2/Ar (vol%) with a constant flow rate of 20 cm^3/min. A molecular sieve cold trap (maintained at 193 K) and a tube filled with KOH were used to block water and CO_2, respectively, before the thermal conductivity detector (TCD).

Transmission electron microscopy (TEM) analyses were performed with a Philips model CM12 electron microscope, operating at 120 kV and directly interfaced with a computer for real-time image processing. The powdered samples were ultrasonically dispersed in isopropyl alcohol, and then a few droplets of the suspension were deposited on a holey carbon support film copper grid. After the solvent evaporated, the specimens were introduced into the microscope column. Several hundred gold particles were measured from each catalyst to obtain a good statistical particle size distribution.

The average size diameter of gold particles in the various samples was calculated using the following formula:

$$\bar{d} = \frac{\sum n_i d_i}{n_i},$$

where n_i is the number of gold particles of diameter d_i.

2.3. Catalytic activity

The catalytic experiments were carried out at atmospheric pressure under H_2 flow, at 333 K, in a 100 ml four-necked batch reactor fitted with a reflux condenser, dropping funnel, thermocouple, and magnetic stirrer head coupled with a gas stirrer (model MRK 1/20-BR; Premex Reactor). This gas stirrer was used to optimize hydrogen transfer from the gas to the liquid phase. The catalyst (weight 0.5–1 g; particle size = 160–200 mesh) was added to 25 ml of solvent and treated at 343 K for 1 h under gaseous H_2. The substrate (6×10^{-4} mol) was injected through one arm of the flask. The reaction mixture was stirred at 700 rpm. The benzalacetone (purity 99.8%) was supplied by ACROS. The progress of the reaction was followed by sampling a sufficient number of microsamples and analyzing them by gas chromatography–mass spectroscopy, using a Shimadzu model GC-QP5000 instrument. The reaction products were separated on a CP-WAX capillary column (1.20 µm, 60 m, 0.32 mm).

Catalytic activity was measured in terms of initial rates and calculated from the slope of the curves conversion versus time (t) at $t = 0$. Selectivities were calculated by $S_i = C_i / \sum C_p$, where C_i is the concentration of product I, and C_p is the total concentration of the products. Preliminary tests carried out with varying catalyst amounts (0.2–1.0 g) grain sizes (80–200 mesh), and stirring rates (500–1000 rpm) indicated that under the conditions used, the reaction was carried out in the absence of mass-transfer limitation.

3. Results and discussion

The chemical and microstructural properties of all gold catalysts are reported in Table 1. Gold loading ranged between 2 and 6 wt%. The surface area of the samples varied within a wide range, from 6 to 171 m^2/g.

Table 1
Mean characteristics of gold supported catalysts

Entry	Catalyst	Au (wt%)	Support	S.A. (m^2/g)	Note
1	AF5dp	5.4	Ferrihydrite Fe_5O_8H Goethite FeO(OH) Hematite αFe_2O_3	121	Ref. [7]
2	AF4.4dp(G)	4.4	Goethite FeO(OH)	171	
3	AF3.2dp(M)	3.2	Maghemite γFe_2O_3	43	
4	AF2.7dp(H)	2.7	Hematite αFe_2O_3	6	
5	Au/Fe_2O_3	4.4	Hematite αFe_2O_3	39	"Reference" catalyst, supplied by the World Gold Council, Type C, Lot No. Au/Fe_2O_3 #02–3

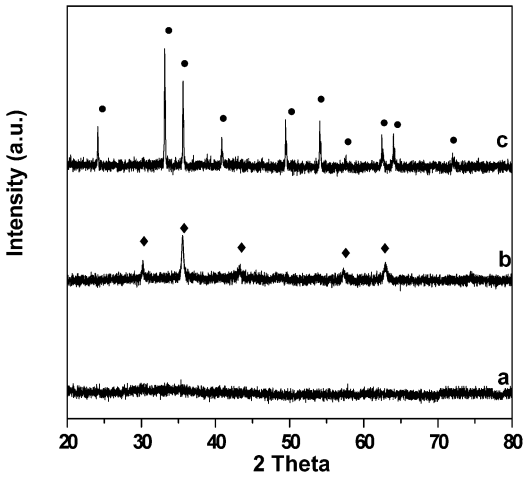

Fig. 1. XRD spectra of the iron oxide supports: (a) goethite FeO(OH), (b) maghemite γFe_2O_3, (c) hematite αFe_2O_3. (◆) Maghemite; (●) hematite.

Characterization of the commercial supports by XRD (Fig. 1, a–c) showed that goethite was amorphous, whereas maghemite and hematite were in crystalline form. XRD analysis of the iron oxy-hydroxide support (Fig. 2a) showed hematite as the main crystallographic phase, followed by goethite and ferrihydrite. The addition of gold on commercial goethite, maghemite, and hematite produced no structural changes in the iron oxide phase on the XRD spectra with respect to that of the parent supports. When gold was deposited on the iron oxy-hydroxide support, the ferrihydrite phase almost disappeared (Fig. 2b). It is likely that during the deposition of gold, ferrihydrite was transformed into the more ordered hematite phase [16].

Table 1 also reports the chemical and structural data for the Au/Fe_2O_3 reference catalyst supplied by the World Gold Council. On this catalyst, prepared according to the coprecipitation method of Haruta, the support was present as crystalline hematite (Fig. 2c).

3.1. TPR measurements

The reducibility of gold catalysts and of the parent supports was investigated by TPR. Before the TPR measurements, the

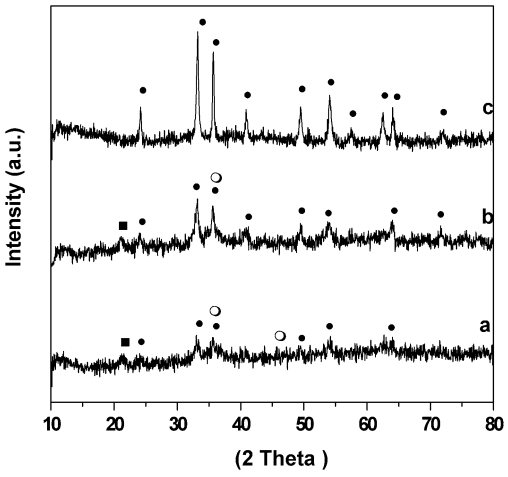

Fig. 2. XRD spectra of the iron oxide supports and related gold catalysts (from Ref. [7]): (a) iron oxy-hydroxide, (b) AF5dp, (c) Au/Fe_2O_3 reference. (■) Goethite; (●) hematite; (○) ferrihydrite.

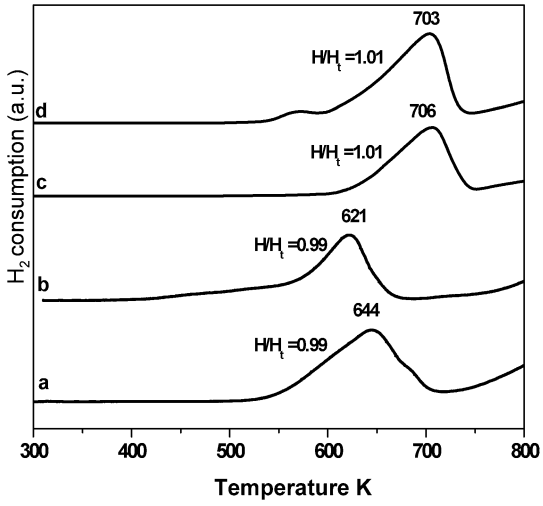

Fig. 3. TPR of iron oxide supports: (a) goethite FeO(OH), (b) maghemite γFe_2O_3, (c) hematite αFe_2O_3, (d) iron oxy-hydroxide. H/H_t is the ratio between the hydrogen consumed, H, and theoretical hydrogen, H_t, which is necessary for the reduction of Fe(III) species to magnetite (Fe_3O_4).

catalysts and the parent supports were suspended in 25 ml of ethanol and reduced under H_2 flow for 1 h at 343 K. This is the same reduction procedure used before the catalytic activity measurements (see Section 2).

Fig. 3 shows the reduction profiles of all iron oxides used as supports. In the temperature range used in this investigation, all of the commercial samples had one peak of reduction (Fig. 3, a–c). The amount of hydrogen consumed, H, calculated from the area under the peak, corresponded to the reduction of Fe(III) species to magnetite (Fe_3O_4). This is outlined from the ratio H/H_t (Fig. 3), where H_t represents the theoretical amount of hydrogen needed for the reduction step of Fe(III) species to Fe_3O_4.

The reduction of FeO(OH) (Fig. 3a) and of γFe_2O_3 (Fig. 3b) occurred at 644 and 621 K, respectively, whereas the reduction of hematite (Fig. 3c) occurred at a higher temperature (706 K). The iron oxy-hydroxide support, formed by a mixture of ferrihydrite, goethite, and αFe_2O_3, showed two overlapping reduction peaks, attributed, from the ratio H/H_t, to the reduction of Fe_2O_3 to magnetite (Fig. 3d). Considering the reduction profiles of commercial goethite and hematite (Fig. 3, a and c), it can be concluded that the reduction profile of the iron oxy-hydroxide support arose from the superimposition of the reduction peaks of the most hydroxilated phases—ferrihydrite and FeO(OH)—that occur at lower temperature, and of the reduction peak of αFe_2O_3.

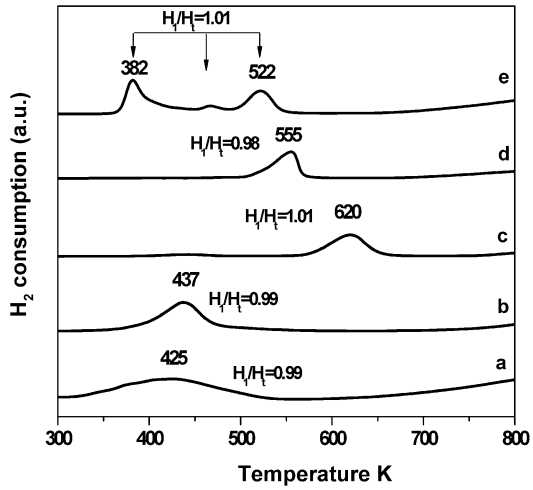

Fig. 4. TPR of iron oxide samples: (a) AF4.4dp(G), (b) AF3.2dp(M), (c) AF2.7dp(H), (d) Au/Fe_2O_3 reference, (e) AF5dp. H_1/H_t is the ratio between the hydrogen consumed, H_1, and theoretical hydrogen, H_t, which is necessary for the reduction of Fe(III) species to magnetite (Fe_3O_4).

The addition of gold on iron oxides enhances the reducibility of catalysts (Fig. 4, a–e). On all of the catalysts investigated, the ratio between the amount of hydrogen consumed (H_1) and the theoretical amount of hydrogen necessary for the reduction step Fe(III) to Fe_3O_4 (H_t) was close to 1 (Fig. 4, a–e), indicating that gold was under a metallic state. The presence of reduced gold on the Au/Fe_2O_3 reference was obvious, because the sample was calcined at 673 K. On the other samples, the reduction of gold likely occurred during pretreatment of the catalysts in H_2 at 343 K. TPR results suggest that the presence of gold mainly enhances the partial reduction of Fe(III) species to magnetite.

On gold supported on goethite and maghemite (Fig. 4, a and b), the reduction peak was shifted by ≈200 K at a lower temperature with respect to that of the supports, whereas on gold supported on hematite (Fig. 4c), the temperature shift was less pronounced (≈90 K). For comparison, the TPR profile of the reference catalyst is also reported (Fig. 4d). It can be seen that the reduction temperature was lower than that observed on the AF2.7dp(H) sample (Fig. 4c). This difference may be due to the greater amount of gold present in the reference sample. It has been reported that the reduction temperature of Fe_2O_3 to Fe_3O_4 decreases with increasing gold loading [17]. Similar behavior was also observed by Andreeva [18] in a TPR study of Au supported on CeO_2 catalysts. In addition, the increase in surface area from AF2.7dp(H) to the Au/Fe_2O_3 reference (Table 1) may also contribute to the shift to a lower-temperature

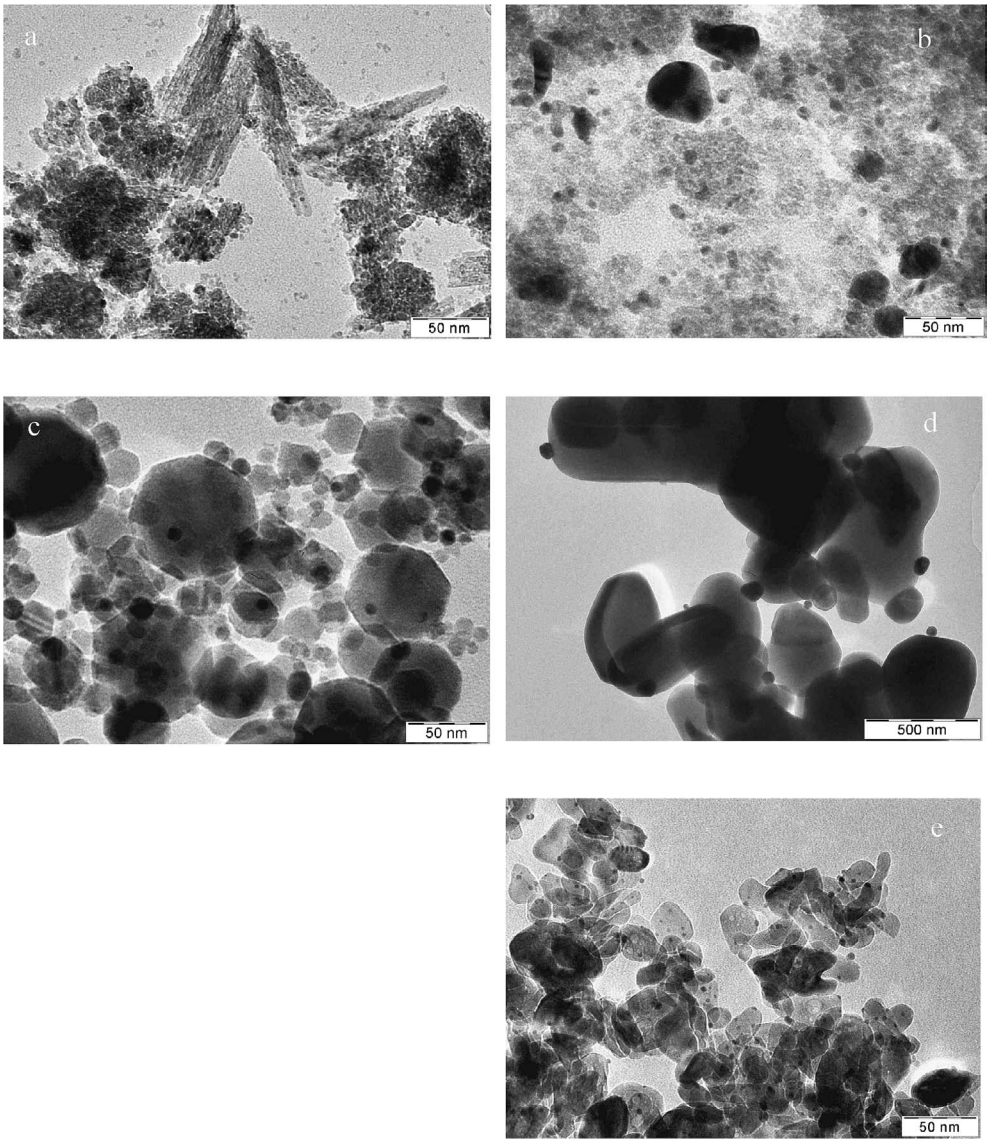

Fig. 5. TEM microphotographs of gold supported catalysts: (a) AF5dp (from Ref. [7]), (b) AF4.4dp(G), (c) AF3.2dp(M), (d) AF2.7dp(H), (e) Au/Fe_2O_3 reference (from Ref. [7]).

reduction peak observed on Au/Fe_2O_3. The influence of surface area on the reduction temperature of Fe_2O_3 to magnetite has been pointed out by Neri et al. [17], who reported that on a similar iron oxide phase, an increase in surface area causes a shift to lower reduction temperatures.

TPR of gold supported on iron oxy-hydroxide support (AF5dp) showed a more complex profile (Fig. 4e). Two main reduction peaks were seen at 382 and 522 K, together with a less intense peak at 467 K. It can be argued that the peak at the lowest temperature is related to the reduction of the most reducible hydroxilated iron oxide phase [FeO(OH) and ferrihydrite], whereas the peak at the higher temperature is related to the reduction of the less reducible hematite.

3.2. TEM measurements

TEM microphotographs of the catalysts reduced for 1 h in H_2 at 343 K in ethanol are shown in Figs. 5a–5e. As is clearly visible, significant differences exist in both the microstructure and particle size of the supports; therefore, we first give a brief description of the morphology of the different iron oxide supports. On AF5dp catalyst (Fig. 5a), the support exhibited a heterogeneous microstructure, likely due to the presence of different crystalline phases. This is in agreement with the XRD results (Fig. 2b) showing the presence of various iron oxide mixed phases, namely ferrihydrite, goethite, maghemite, and hematite.

TEM analysis of the AF4.4dp(G) catalyst (Fig. 5b), prepared using commercial goethite, showed instead the homogeneous structure of the support consisting of aggregates of almost round and very small (around 3–5 nm in diameter) goethite particles. Fig. 5c shows the AF3.2dp(M) catalyst prepared using a commercial well-crystallized maghemite support with a hexagonal closely packed morphology and a very wide particle size distribution (10–100 nm). TEM micropho-

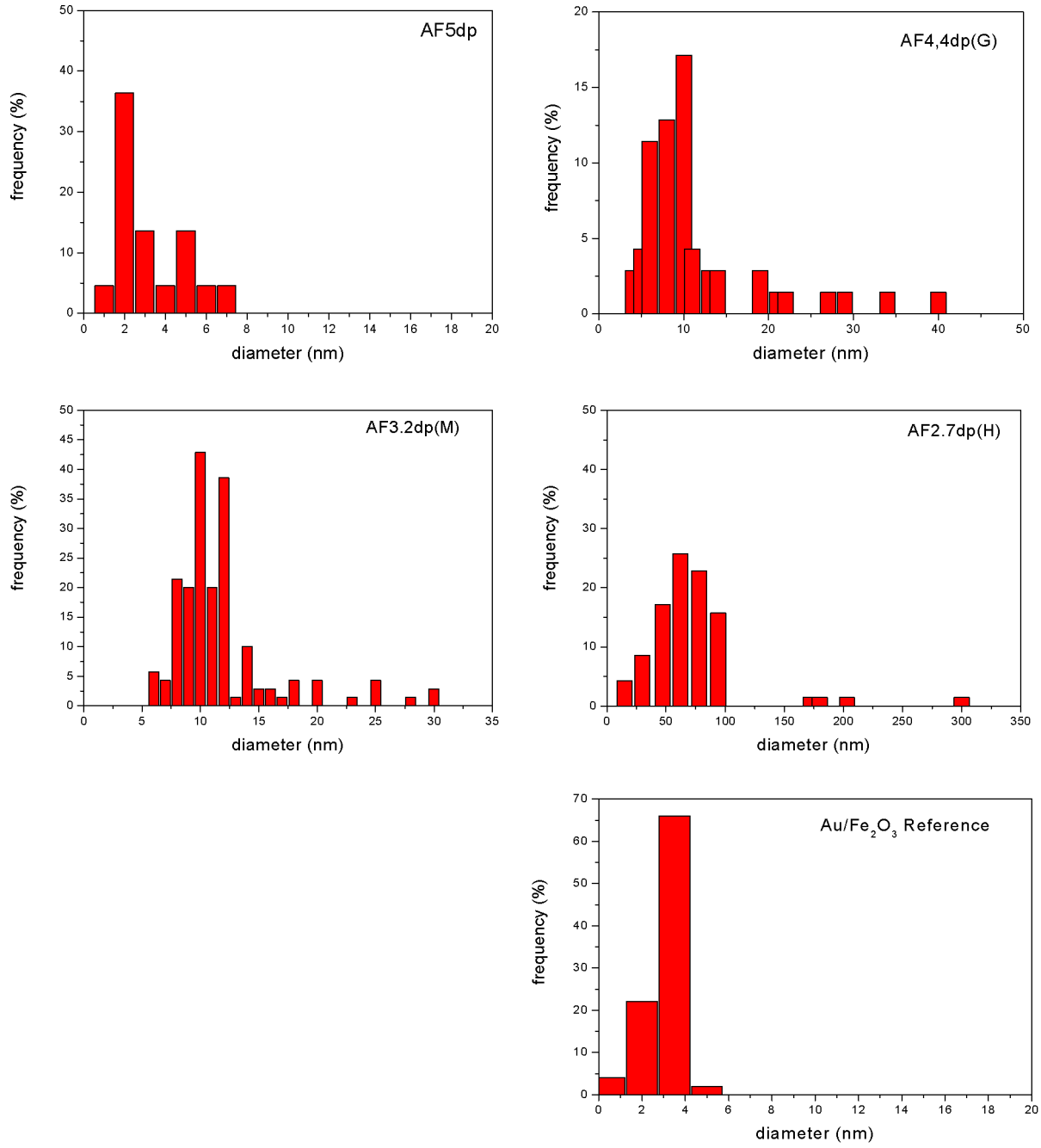

Fig. 6. Particle size distribution of gold supported catalysts.

tographs reported in Figs. 5d–5e refer to gold catalysts supported on hematite. AF2.7dp(H) catalyst (Fig. 5d) was prepared by us using a commercial hematite as support and exhibited the characteristic morphology of sintered powders, likely due to the high temperature of the preparation process. The particles of the hematite support on the Au/Fe_2O_3 reference catalyst were much smaller (around 10–50 nm diameter).

The particle size distribution and mean particle diameter of gold are reported in Fig. 6 and Table 2, respectively. The AF5dp sample exhibited small gold particles and a narrow particle size distribution. On the AF4.4dp(G) and AF3.2dp(M) samples, a monomodal distribution centered around 10 nm was obtained. A low frequency of gold particles larger than 20 nm was also found in both samples (Fig. 6).

TEM microphotographs of gold catalysts supported on hematite, AF2.7dp(H), and the Au/Fe_2O_3 reference (Figs. 5d and 5e) exhibit well-isolated gold crystallites of varying size. The Au/Fe_2O_3 reference catalyst had very small gold particles and a narrow particle size distribution centered around 3.7 nm (Fig. 6). A significant increase in gold particle size can be observed when the noble metal was supported on commercial hematite. Indeed, on the AF2.7dp(H) sample, large gold particles (diameter 10–100 nm) are seen.

Table 2
Catalytic activity and products distribution in the hydrogenation of benzalacetone on gold catalysts

Entry	Catalyst	Au (wt%)	Mean gold particle size d (nm)	V_i (mol/g_{Au} s) × 10^7	Selectivity (%) (conversion ⩾90%)[a]		
					SK	UA	SA
1	AF5dp	5.4	3.2 ± 2.0	28.7	18	**59**	23
2	AF4.4dp(G)	4.4	11.4 ± 3.0	24.2	14	**64**	21
3	AF3.2dp(M)	3.2	10.0 ± 2.0	9.2	31	**56**	13
4	AF2.7dp(H)	2.7	62.0 ± 10.0	3.7	94	**6**	2
5	Au/Fe_2O_3[b]	4.4	3.7 ± 0.9	1.0	77	**20**	3

[a] SK = saturated ketone; UA = unsaturated alcohol; SA = saturated alcohol.
[b] Gold reference catalyst, Type C, Lot No. Au/Fe_2O_3 #02–3.

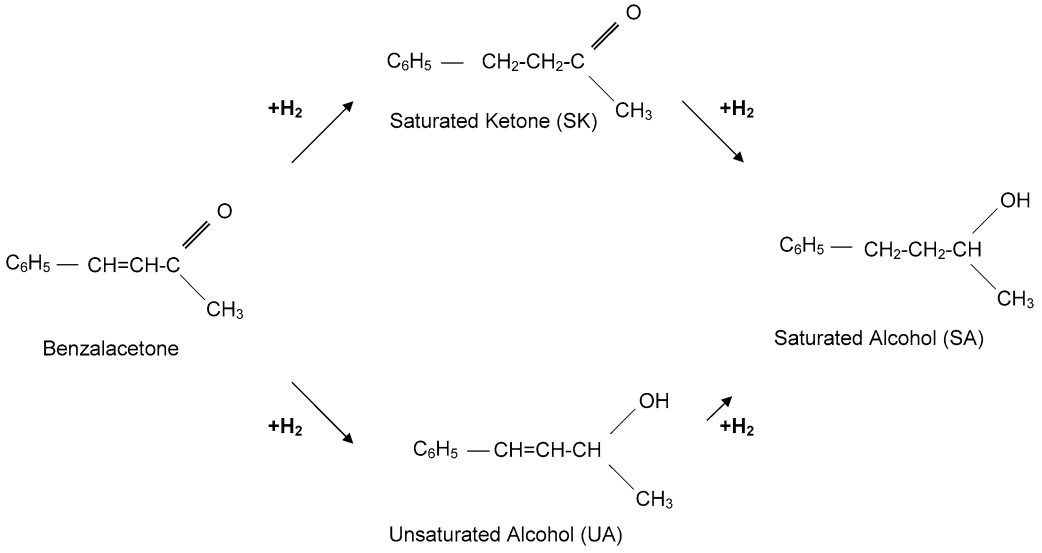

Scheme 1. Reaction pathways in the hydrogenation of benzalacetone.

3.3. Catalytic activity

On all gold preparations, the hydrogenation of benzalacetone (C_6H_5–CH=CH–CO–CH_3) led to the formation of saturated ketone (SK) (C_6H_5–CH_2–CH_2–CO–CH_3) from hydrogenation of the conjugated C=C bond and of UA (C_6H_5–CH=CH–CHOH–CH_3) from hydrogenation of the C=O bond through two parallel reactions (see Scheme 1). At high conversion of the substrate (>80%), saturated ketone was further hydrogenated to the corresponding saturated alcohol (SA) (C_6H_5–CH_2–CH_2–CHOH–CH_3). Hydrogenation of the UA hardly occurred even when the conversion of benzalacetone approached 100%.

Complete hydrogenation of benzalacetone was achieved on all of the catalysts. The catalytic activity of gold preparations, expressed as the initial rate of hydrogenation of benzalacetone per gram of gold, is reported in Table 2. It can be seen that catalytic activity increased with increasing gold content on all gold catalysts except the Au/Fe_2O_3 reference.

The low activity of reference with respect to the catalysts with similar gold loadings (entries 1 and 5) can arise from the different sample pretreatments. The Au/Fe_2O_3 reference was calcined at 773 K, whereas our catalysts were reduced under very mild conditions (343 K for 1 h in ethanol). Calcination of the solid was detrimental to catalytic activity in the hydrogenation of benzalacetone [7]. No correlations between catalytic activity and mean gold particle size can be drawn from our data. Uncalcined catalysts with similar gold particle size (entries 2 and 3) showed very different catalytic activity.

Table 2 also reports the product distribution, at high conversion level (⩾90%), on all of the catalysts investigated. The highest selectivity toward formation of UA was obtained on gold catalysts supported on goethite, AF4.4dp(G), on the iron oxy-hydroxide support, AF5dp, and on the maghemite, AF3.2dp(M). The Au/Fe_2O_3 reference showed intermediate selectivity, whereas AF2.7 dp(H) showed the lowest selectivity to UA.

The selectivity toward the formation of UA is not correlated with the gold particle size. As is shown in Table 2, AF4.4dp(G) and AF3.2dp(M) had a similar mean gold particle size but different selectivity toward the formation of UA. On AF4dp(G) the selectivity was 64%, whereas on AF3.2dp(M) it decreased to 56%.

A more significant decrease in selectivity toward the formation of UA was observed passing from AF5dp to the Au/Fe_2O_3 reference. The mean gold particle size was very close on these two catalysts, but the selectivity was almost 3 times higher on AF5dp than on the Au/Fe_2O_3 reference. These findings suggest that the selectivity toward hydrogenation of the conjugated C=O bond does not depend on gold particle size, but varies

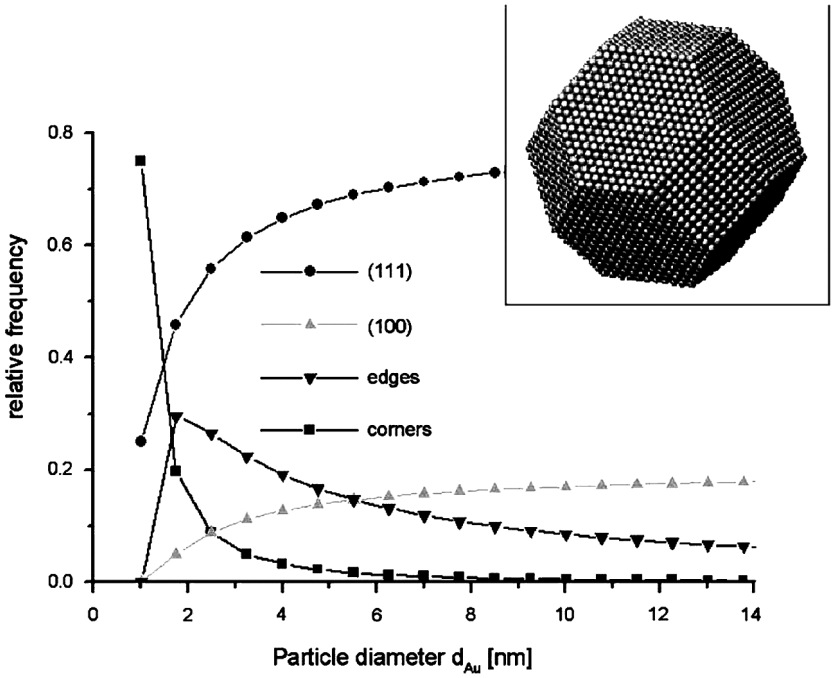

Fig. 7. Dependence of relative amounts of surface sites on particle diameter of cuboctahedron gold particles (from Ref. [24]).

with the structural characteristics of the support ranking in the following order:

FeO(OH)
> iron oxy-hydroxide [ferrihydrite, FeO(OH), αFe_2O_3]
> $\gamma Fe_2O_3 \gg \alpha Fe_2O_3$.

However, it should be also pointed out that on gold supported on hematite (entries 4 and 5), selectivity to UA decreased from 20 to 6% when gold particle size increased from 3.7 to 62 nm.

Assuming that the shape of the fcc metallic gold of nanometer size is cuboctahedral, the relative amount of surface, edge, and corner atoms hardly changed for particles >3 nm in diameter (Fig. 7). In consideration of the fact that the gold particle size of the hematite-supported catalysts varies from 3.7 to 62 nm, it is likely that a pure geometric effect cannot explain the decreased selectivity with increasing of particle size. Moreover, Rao et al. [19] found that the Au $4f_{7/2}$ binding energy of gold clusters dispersed on amorphous graphite with different diameters (0.6–10 nm) increased significantly with respect to the value of bulk gold (84.0 eV) with cluster diameter $< \approx 2$ nm [19]. For clusters >2 nm, the binding energy corresponds to that of the bulk value. Therefore, for gold catalysts supported on hematite > 3 nm in diameter, an electronic effect of gold on the selectivity to UA is unlikely.

The affect of gold particle size on hydrogenation of the conjugated C=O bond has been mainly investigated in the hydrogenation of α,β-unsaturated aldehydes, and literature data vary and are somewhat controversial. Claus et al. [2,20] reported that the selectivity to crotyl alcohol in hydrogenation of acrolein on Au/TiO_2 and Au/ZrO_2 increases with increasing gold particle size. These authors concluded that the C=O group is preferentially activated on gold sites of high coordination (face atoms), whereas sites of low coordination, mostly present on small particles as corners and edges, strongly favors the activation of the C=C group. A marked increase in selectivity toward UA with increasing metal particle size also was observed in studies on crotonaldehyde hydrogenation and prenal hydrogenation over Pt catalysts [21–24].

Mohr et al. [25] identified the edge of gold nanoparticles as active sites in the hydrogenation of acrolein through the decoration of gold particle faces by a second metal, leaving the edge position free. This conclusion is clearly in contradiction to the earlier assumption. Zanella et al. [5] reported that the hydrogenation of the C=O group of the crotonaldehyde on Au/TiO_2 is almost independent of gold particle size when it varies in the range 1.7–8.7 nm.

In summary, in this work the selectivity toward the formation of UA was found to be higher when gold is dispersed on goethite, iron oxy-hydroxide support (a mixture of ferrihydrite, goethite, and hematite), and maghemite and to drop when gold is dispersed on hematite. These differences cannot be due to a pure size effect (electronic and/or geometric) of gold particles; the support should play a significant role in the catalytic properties of the catalysts. From the results reported in Table 2, is clear that the surface area of the catalysts does not influence the product distribution in the hydrogenation of benzalacetone. Indeed, catalysts with similar surface areas—Au/Fe_2O_3 reference and AF3.2dp(M)—showed large differences in selectivity toward the hydrogenation of C=O.

Mohr et al. [20] demonstrated that activity and selectivity in the hydrogenation of acrolein on gold depends not only on particle size, but also on other factors involved in gold morphology, such as the degree of rounding of particles and the portion of multiple twinned gold particles. In this respect, the nature of the support apparently strongly affects the morphology of gold particles.

Radnik et al. [26] also reported that on SiO_2 and TiO_2, the gold particles are nearly spherical, whereas on the other supports, such as ZrO_2 and ZnO, extended facets of the gold surface are visible. On the nearly spherical gold particles, a higher number of low-coordination sites are present on the surface with respect to the faceted ones. From the TEM microphotographs shown in Fig. 5, we cannot evaluate whether changes in the morphology of gold particles were induced by the iron oxide support. This point merits further investigation through high-resolution TEM analysis of the samples.

Another possibility is that the support induces a modification of the electron density of the metal, which in turn leads to changes in its adsorption properties. Claus and co-workers [26,27] observed, by means of electron paramagnetic spectroscopy and X-ray photoelectron spectroscopy, that the reduction in H_2 of gold supported on TiO_2 and ZrO_2 catalysts at 773 and 573 K, respectively, causes a partial reduction of the support and an increased electron density on gold. When the reduced samples are stored to ambient atmosphere, reoxidation of the support occurs [27]. The increased electron density of the metal on reduction has been explained claiming an electron transfer from the reduced support to the metal [27]. It has been suggested that the presence of electron-enriched gold particles favors selective hydrogenation of C=O in the hydrogenation of α,β-unsaturated aldehydes [2]. On these sites, the binding energy of the C=C bond should decrease via an increase of the four-electron interaction, whereas back-bonding with the π^* C=O orbital should be favored, so that the hydrogenation of the C=O group should be enhanced over that of the C=C group [2].

Neri et al. [28] reported that gold supported on iron oxide thick films, prepared by coprecipitation and calcined at different temperatures, can be used as sensors for reducing gas as CO at room temperature. The proposed mechanism for the detection of CO on samples calcined at temperatures $>100\,^{\circ}C$, where gold is in the metallic state, involves the oxidation of the gas by adsorbed oxygen and/or lattice oxygen of the n-type semiconductor oxide. This causes an increase of the electrical conductivity of the bulk, that is, an increase in the electron density of the bulk [28]. In our case, it can be argued that during the reduction of the catalyst in situ before the reaction, besides the reduction of gold(III) to metallic gold, the oxidation of the H_2 by the lattice oxygen of the support also can occur, leading to a reduction of the support and an increased electron density of the bulk. Under these conditions, electron transfer from the bulk to the anchored gold metal is likely to occur.

Considering that the catalyst prereduction was carried out at low temperature (343 K), we expected the degree of reduction of the support (i.e., the increased electron density of the bulk) to be higher on catalysts with lower reduction temperatures and to decrease with increasing reduction temperature. Thus, we tried to make a correlation between the selectivity toward the formation of UA in the hydrogenation of benzalacetone and the reducibility (in terms of T_{max} of reduction) of the catalysts. For the sample AF5dp, which had two main reduction temperatures (383 and 522 K; Fig. 4e), the lower reduction temperatures have been taken into account. The reason for this choice arises from

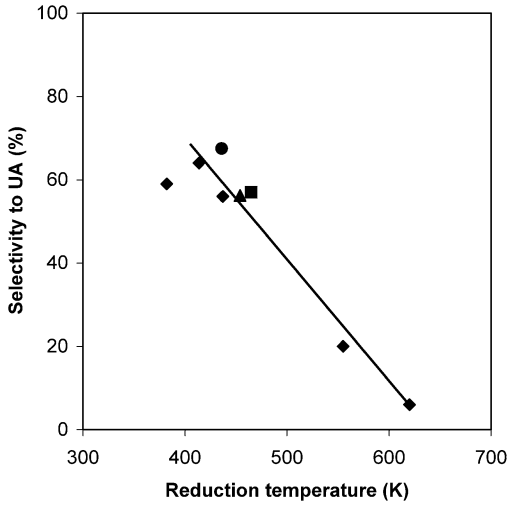

Fig. 8. Relationship between the selectivity towards the unsaturated alcohol, measured at conversion $\geqslant$90%, and T_{max} of reduction of catalysts. (◆) Catalysts of this work, and (▲) AF3.1, (■) AF5.3, (●) AF16.6 from Ref. [7].

the fact that the in situ catalyst prereduction was carried out under mild conditions; therefore, it is reasonable to consider that the reduction of the support will affect mainly the most reactive fraction—that with the lower reduction temperature. Note that the selectivity to UA reported in Fig. 8 was measured at a conversion rate $\geqslant$90%.

Fig. 8 shows that for almost all of the gold catalysts, the selectivity toward UA increases with decreasing T_{max} of reduction of the catalysts. Only AF5dp deviates slightly from the linear correlation reported in Fig. 8. Within this correlation, we have also included the results obtained in the hydrogenation of benzalacetone on Au/iron oxide catalysts prepared by coprecipitation and reported in a previous work [7]. In that paper it was reported that coprecipitated gold catalysts showed a selectivity toward UA that varied from 56 to 67% and did not depend on gold particle size [7].

Therefore, in Fig. 8 we report selectivity measured on the coprecipitated catalysts, measured at conv $\geqslant$90% versus their reduction temperature. As shown in the figure, the data fit well within this correlation, thus confirming their general validity.

The low selectivity of gold supported on hematite catalysts can be explained by considering their lower reducibility, which in turn leads to a lower increase in the electron density of the bulk. Previously, Neri et al. [28] also found that the increased conductivity of Au supported on hematite on CO detection is much lower than that observed on Au supported on an amorphous iron oxy-hydroxide phase under the same operating conditions.

In addition, looking at the results obtained on gold catalysts supported on hematite, the higher selectivity of the reference catalyst compared with AF2.7dp(H) can be explained by considering the lower temperature of reduction of the former (Fig. 4, c and d). Therefore, the more reducible the catalyst, the higher the selectivity toward the hydrogenation to C=O. As suggested by Claus and co-workers [26,27], the reason for this could lie in the increased extent of electron transfer from the reduced support to the gold metal, creating a more electron-

Table 3
Initial rate of hydrogenation, V (mol/(s g_{Au})) of the saturated ketone 4-phenyl-butan-2-one, $C_6H_5CH_2–CH_2–COCH_3$, and of styrene $C_6H_5CH=CH_2$

Catalyst	Mean gold particle size d (nm)	$V_{C_6H_5CH_2–CH_2–COCH_3}$ (mol/g_{Au} s))×10^7	$V_{C_6H_5CH=CH_2}$ (mol/(g_{Au} s))×10^7
AF5dp	3.2 ± 2.0	6.9	0.5
Au/Fe_2O_3[a]	3.7 ± 0.9	0.5	0.4

[a] Gold reference catalyst, Type C, Lot No. Au/Fe_2O_3 #02–3.

enriched gold, on which the hydrogenation of C=O should be favored over that of C=C.

Consideration should be given to the behavior of the AF5dp catalyst, which shows a slight deviation from the linear correlation represented in Fig. 8. In our opinion this behavior can arise from the microstructural inhomogeneity of the support containing both high-reducible [ferrihydrite and FeO(OH)] and low-reducible (αFe_2O_3) iron oxide phases. Therefore, only gold dispersed on the highly reducible phase(s) acts as the most selective site for the hydrogenation of C=O, whereas gold dispersed on the less-reducible αFe_2O_3 provides a lower contribution to selectivity. This possibility requires further investigation, however.

It should be highlighted that the presence of a reducible support by itself is not sufficient to enhance the hydrogenation rate of C=O with respect to the C=C bond in the hydrogenation of benzalacetone; both gold and reducible iron oxides are necessary. In a previous work [7] we reported that in the hydrogenation of benzalacetone carried out on a Ru catalyst prepared by dispersing colloids of metallic ruthenium on the same support used to prepare the AF5dp catalyst, the main reaction product was saturated ketone and selectivity toward the formation of UA was <2%, whereas on AF5dp the selectivity toward UA was 59%. TPR analysis of Ru catalyst showed that the reduction of Fe_2O_3 to Fe_3O_4 occurred at 447 K. From the correlation reported in Fig. 8, a selectivity >50% should be expected on this catalyst. The lower selectivity obtained (2%) confirms that gold has an intrinsic specificity toward the selective hydrogenation of conjugated C=O and that the catalytic behavior of gold on iron oxide catalysts arises from a synergetic effect between the two constituents.

We also investigated the influence of the reducibility of the catalysts on the hydrogenation of the unconjugated C=C and C=O bond, carrying out hydrogenation of the saturated ketone, 4-phenyl-butan-2-one ($C_6H_5CH_2–CH_2–CO–CH_3$), and of styrene ($C_6H_5CH=CH_2$) on AF5dp and Au/Fe_2O_3 reference catalysts with different reducibility (Fig. 4, d and e). As shown in Table 3, the initial rate of hydrogenation of the single C=O bond (saturated ketone) is higher on AF5dp with respect to Au/Fe_2O_3, whereas the initial rate of hydrogenation of the C=C single bond (styrene) is similar on both catalysts. These results suggest that increasing the reducibility of the catalyst increases selectivity toward the formation of the UA due to enhancement of the hydrogenation rate of C=O.

Taking into account the results of this work and in accordance with our earlier findings, we can conclude that gold is a metal with a high intrinsic selectivity toward the hydrogenation of C=O. The intrinsic selectivity of gold can be due to the adsorption mode of the conjugated systems on this metal. It has been previously suggested that among the different adsorption modes of the conjugated systems, gold is likely a metal on which the 1,2-C=O adsorption mode (which in turn leads to the formation of UA) is preferred over the 1,4-C=C–C=O adsorption mode, which is responsible for the formation of saturated carbonyl compounds. The selectivity toward the formation of UA is strongly influenced by the support and increases with increasing reducibility of the support. In agreement with findings of Claus and co-workers [26,27], it can be suggested that an electron transfer from the reduced support to the metal creates more electron-enriched gold particles on which back-bonding with the π^* C=O orbital is favored, so that hydrogenation of the C=O group is greater than that of the C=C group. However, the possibility that the enhanced selectivity is favored through a cooperative effect of special Fe(III) or Fe(II) sites and more negatively charged gold nanoparticles present near the reduced support cannot be ruled out.

4. Conclusions

From the results reported in this paper, it can be concluded the selectivity toward hydrogenation of the conjugated C=O bond of benzalacetone is little influenced by gold particle size, but is strongly influenced by the support. A good correlation has been found between the reducibility of the support and the selectivity toward the hydrogenation of conjugated C=O. This correlation has been explained by an electron-transfer mechanism from the reduced support to the metal, which creates electron-enriched gold particles on which strongly enhanced hydrogenation of C=O occurs. Nonetheless, the possibility that the enhanced selectivity is favored through a cooperative effect of special Fe(III) or Fe(II) sites and more negatively charged gold nanoparticles present near the reduced support cannot be ruled out.

References

[1] C. Mohr, H. Hofmeister, M. Lucas, P. Claus, Chem. Eng. Technol. 3 (2000) 324.
[2] P. Claus, A. Brückner, C. Mohr, H. Hofmeister, J. Am. Chem. Soc. 122 (2000) 11430.
[3] J.E. Bailie, H.A. Abdullah, G.J. Hutchings, et al., Phys. Chem. Chem. Phys. 3 (2001) 4113.
[4] C. Milone, M.L. Tropeano, G. Gulino, G. Neri, R. Ingoglia, S. Galvagno, J. Chem. Soc., Chem. Commun. (2002) 868.
[5] R. Zanella, C. Louis, S. Giorgio, R. Touroude, J. Catal. 223 (2004) 328.
[6] C. Milone, R. Ingoglia, M.L. Tropeano, G. Neri, S. Galvagno, J. Chem. Soc., Chem. Commun. (2003) 868.
[7] C. Milone, R. Ingoglia, A. Pistone, G. Neri, F. Frusteri, S. Galvagno, J. Catal. 222 (2004) 348.
[8] J. Kaspar, M. Graziani, G. Picasso Escobar, A. Trovarelli, J. Mol. Catal. 72 (1992) 243.
[9] M. Gargano, V. D'Orazio, N. Ravasio, M. Rossi, J. Mol. Catal. 58 (1990) L5.
[10] S.N. Coman, V.I. Parvulescu, M. De Bruyn, D.E. De Vos, P. Jacobs, J. Catal. 206 (2002) 218.
[11] M. De Bruyn, S. Coman, R. Bota, V.I. Parvulescu, D.E. De Vos, P.A. Jacobs, Angew. Chem. Int. Ed. 42 (2003) 5333.
[12] V. Ponec, Appl. Catal. A: Chem. 149 (1997) 27.

[13] P. Gallezot, D. Richard, Catal. Rev. Sci. Eng. 40 (1&2) (1998) 81.
[14] M. Haruta, CATTECH 6 (3) (2002) 102.
[15] F.E. Beamish, J.C. van Loon, Analysis Noble Metals, Academic Press, New York, 1977.
[16] U. Schewertmann, R.M. Cornell, Iron Oxides in the Laboratory: Preparation and Characterization, VCH, Weinheim, 1991.
[17] G. Neri, A.M. Visco, S. Galvagno, M. Panzalorto, Thermochim. Acta 329 (1999) 39.
[18] D. Andreeva, Gold Bull. 35 (2002) 82.
[19] C.N.R. Rao, A.K. Santra, V. Vijayakrishnan, Top. Catal. 1 (1994) 25.
[20] C. Mohr, H. Hofmeister, P. Claus, J. Catal. 213 (2003) 86.
[21] M. English, A. Jentys, J.A. Lercher, J. Catal. 166 (1997) 25.
[22] Y. Berthier, C.M. Pradier, Bull. Soc. Chim. Fr. 134 (1997) 773.
[23] T. Birchem, C.M. Pradier, Y. Berthier, G. Cordier, J. Catal. 146 (1994) 503.
[24] C.M. Pradier, T. Birchem, Y. Berthier, G. Cordier, Catal. Lett. 29 (1994) 371.
[25] C. Mohr, H. Hofmeister, J. Radnik, P. Claus, J. Am. Chem. Soc. 125 (2003) 1905.
[26] J. Radnik, C. Mohr, P. Claus, Phys. Chem. Chem. Phys. 5 (2003) 172.
[27] S. Schimpf, M. Lucas, C. Mohr, U. Rodemerck, A. Bruckner, J. Radnik, H. Hofmeister, P. Claus, Catal. Today 72 (2002) 63.
[28] G. Neri, A. Bonavita, C. Milone, S. Galvagno, Sens. Actuators B 93 (2003) 402.